Carbohydrate Polymers 119 (2015) 35–43

Contents lists available at ScienceDirect

Carbohydrate Polymers

journal homepage: www.elsevier.com/locate/carbpol

Native and structurally modified gum arabic: Exploring the effect of the gum's microstructure in obtaining electroactive nanoparticles

Patricia A. Cornelsen[a], Ronaldo C. Quintanilha[a], Marcio Vidotti[a], Philip A.J. Gorin[b], Fernanda F. Simas-Tosin[a,b], Izabel C. Riegel-Vidotti[a,*]

[a] Grupo de Pesquisa em Macromoléculas e Interfaces, Departamento de Química, Universidade Federal do Paraná—UFPR, CxP 19081, CEP 81531-980 Curitiba, PR, Brazil
[b] Departamento de Bioquímica e Biologia Molecular, Universidade Federal do Paraná—UFPR, CxP 19046, CEP 81531-980, Curitiba, PR, Brazil

ARTICLE INFO

Article history:
Received 15 July 2014
Received in revised form 2 November 2014
Accepted 3 November 2014
Available online 26 November 2014

Keywords:
Gum arabic
Structural modification
Polyaniline nanoparticles
Electroactive properties

ABSTRACT

Electroactive nanoparticles combining gum arabic (GA) and polyaniline (PANI) were prepared by chemical synthesis. The gum consists of highly branched anionic polysaccharides with some protein content. GA was structurally modified by Smith controlled degradation, in order to reduce its degree of branching (GAD), aiming the elucidation of the relationship between the structure and the properties of complex polysaccharides. The modification was studied by SEC, GC–MS, ^{13}C NMR and colorimetric methods. GAD has lower molecular mass, lower degree of branching and lower uronic acid content. Besides it is enriched in galactose and protein when compared with GA. The obtained composites (GA-PANI and GAD-PANI) were thoroughly characterized. Although the use of both polysaccharides (GA and GAD) produced highly stable electroactive nanoparticles, the best combination of properties was achieved for GA-PANI. The sample GAD was not able to prevent the occurrence of crosslinking between PANI chains, possibly due to its lower microstructural complexity which diminishes the occurrence of hydrogen bonds between the polymers.

1. Introduction

Combining conducting and natural polymers is of interest considering the many possible applications. The aim is to attain the good electrochemical performance of the intrinsically conducting polymers (ICPs) with the biodegradability and biocompatibility of natural polymers (Petrov, Georgiev, Momekova, Momekov, & Tsvetanov, 2010; Shi, Phillips and Yang, 2013). Also, hydrophilic polymers play a role on the stabilization and processing of ICPs in aqueous medium (Stejskal & Sapurina, 2004). In this way, the as-formed new materials are very promising for biomedical applications, mainly as biosensors (Ates, 2013; Janáky & Visy, 2013).

Gum arabic (GA) is the name commonly given to the gum exudated from the trunks and branches of acacia trees. Commercially, it is obtained from the species *Acacia senegal* and *Acacia seyal*, growing mainly in the African countries. GA is a complex polysaccharide, composed of highly branched molecules containing neutral (Gal, Ara, and Rha) and acidic monosaccharides (GlcA and 4Me-GlcA) and low and high molecular mass protein fractions (Williams & Phillips, 2000; Tischer, Gorin, & Iacomini, 2002; Grein et al., 2013). Typically, GA is used as emulsifier and colloidal stabilizer and as nutritional component in food industry (Islam, Phillips, Sljivo, Snowden, & Williams, 1997; Wang, Wang, Dong, Adhikaric, & Shid, 2011). GA is highly soluble in water and displays properties that depend on its molecular characteristics such as molecular mass, degree of branching, protein content as well as the relative amount of uronic acids in its composition. Schematically, Fig. 1A shows the main monosaccharides present in GA (Ferrier & Collins, 1972; Duffus & Duffus, 1984; Cipriani, Mellinger, Gorin, & Iacomini, 2004).

There are some strategies to tune up the GA properties by modifying either its molecular architecture or its composition. Controlled Smith degradation is a method originally proposed for the structural elucidation of carbohydrates. The first step of the procedure is periodate oxidation, which promotes the cleavage of *vic*-glycols linkages with the formation of two aldehydic groups (Hay, Lewis, & Smith, 1965). Therefore, monosaccharides that do not possess adjacent hydroxyl groups are not oxidized by periodate. At the second step, the aldehydic groups are reduced with sodium borohydride to give the corresponding alcohol, which are cleaved by a mild acid hydrolysis at the last step of the procedure.

* Corresponding author. Tel.: +55 41 33613184; fax: +55 41 33613186.
E-mail address: izabel.riegel@ufpr.br (I.C. Riegel-Vidotti).

http://dx.doi.org/10.1016/j.carbpol.2014.11.020
0144-8617/

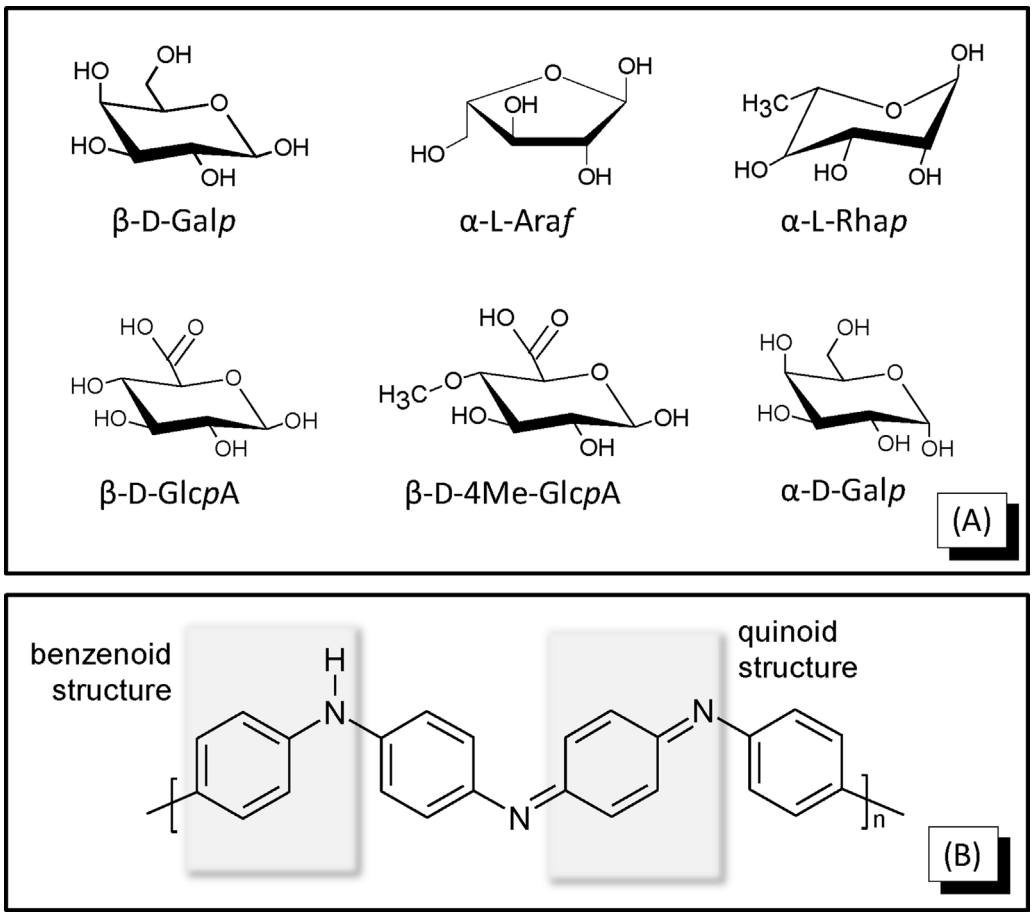

Fig. 1. (A) Main monosaccharides present in gum arabic and (B) molecular structure of polyaniline (PANI) in its emeraldine salt form, showing the benzenoid and quinoid segments.

The monosaccharide units that are not oxidized by periodate are more stable to mild acid hydrolysis (Hay et al., 1965; Goldstein, Hay, Lewis, & Smith, 1965). Therefore, the main factor responsible for controlling the degradation is the chemical structure of the polysaccharide. However, other variables such as conformational accessibility, concentration of oxidizing agent, and the time of oxidation may also influence the degradation results.

Among the ICPs, polyaniline (PANI) is of great interest since it is very stable under atmospheric ambient and can easily be synthesized by many routes, such as chemical, interfacial, emulsion, electrochemical, among others (Palaniappan & John, 2008). A representation of the molecular structure of PANI, in its emeraldine salt (ES) form (partially oxidized) is presented in Fig. 1B. Benzenoid and quinoid rings are observed and the proportion of these two structures indicates the intrinsic electroactivity of the polymer. Besides, many other parameters determine the degree of conductivity such as the amount of charge carries which depends on the doping level, the planarity of π orbitals and also the presence of phenazine structures formed by the inter-chain bonding (or cross-link) which leads to a change on the polymer conformation (Silva, Faria, de Torresi, & Temperini, 2000). In order to extend the ICPs applications, many efforts have been made in order to increase their solubility in aqueous solution, to do so, hydrophilic polymers have long been used to stabilize ICPs in aqueous medium (Stejskal, Kratochvil, & Radhakrishnan, 1993). Among them, some have reported the synthesis of ICPs in the presence of chitosan and heparin (Guo, Glavas, & Albertsson, 2013). In all cases, distinct features of the conducting composites are desired. For example, the presence of heparin provides excellent substrate for cell growth and enhancement of the biodegradability of the materials.

Recently (Quintanilha, Orth, Grein-Iankovski, Riegel-Vidotti, & Vidotti, 2014) our group has reported a simple and straightforward procedure to obtain PANI nanocomposites stable in aqueous media. We have demonstrated that the material integrity is kept by strong hydrogen bonds. This feature was thoroughly studied by the red shift of the N—H band of PANI by FTIR and by the change of amine specific bands in the Raman spectra. Besides, at higher concentrations of GA the hydrogen bonds between amine (from PANI) and hydroxyl groups (from GA) are prevented, indicating that there are an optimal condition, in terms of GA content, to produce good quality nanocomposites.

The objective of the present study is to demonstrate that the molecular characteristics of the stabilizer affect the final properties of PANI composites. For this, polyaniline was chemically synthesized, in aqueous medium, in the presence of gum arabic in its native form (GA) and structurally modified (GAD) by controlled Smith degradation procedure. GAD has different molecular features when compared with GA. Spectroscopic and electrochemical studies revealed that, accordingly, the composites GA-PANI and GAD-PANI present distinct properties. The results are discussed by taking into account the differences in the molecular characteristics of the polysaccharides, giving special attention to their molecular microstructure. The aim of our work is to contribute to the elucidation of the relationship between structure and properties of complex polysaccharides.

2. Materials and methods

2.1. Materials

Gum arabic (GA) was purchased from Sigma-Aldrich (G9752), which is referred in the label as "gum arabic from acacia tree". The powder was solubilized in water, prepared by a Milli-Q unit (18.2 MΩ.cm, Millipore, USA), dialyzed for 48 h against distilled water through a dialysis membrane (12–14 kDa cut-off) and freeze-dried. Herein GA sample is from the same batch that was employed in a recent work (Grein et al., 2013). Aniline was obtained from Nuclear and distilled prior to use. All other reagents were of analytical grade.

2.2. Controlled Smith degradation

The polysaccharide GA (6.80 g) was dissolved in aqueous $NaIO_4$ solution (0.5610 mol L^{-1}). The solution was kept for 72 h in the dark (Tischer et al., 2002). After, ethylene glycol (5.0 mL) was added and the solution was dialysed (6–8 kDa cut-off) for 24 h against tap water. $NaBH_4$ (2.00 g) was then added and after 24 h the solution was acidified to pH 6.0 with HOAc and dialysed (1200–2000 Da cut-off) for another 24 h. The solution was evaporated to 100 mL, adjusted to pH 2.0 with dil. TFA (trifluoroacetic acid), and kept refluxing for 30 min (Gorin, Horitsu, & Spencer, 1965). Subsequently, the solution was neutralized to pH 5.0 (NaOH 1 mol L^{-1}), dialysed against tap water (1200–2000 Da cut-off) and the retained solution was lyophilized, giving the sample GAD (23.25% yield).

2.3. GAD molecular mass and homogeneity determination

Molecular parameters, $\bar{M}_w$ and polydispersity ($PD = \bar{M}_w/\bar{M}_n$ were determined using a Viscotek GPC/SEC equipment, Model 270 Triple Detector – refractive index (RI), viscosity concentration and light scattering (LS) detectors – equipped with a Shodex OHPak SB-806 HQ GPC aqueous column–plate number ≥12,000, exclusion limit 20,000,000 (Pullulan) and attached to an UV detector. Injections were run at 30 °C and at a 0.4 mL min^{-1} flow rate. GA or GAD (2.00 g L^{-1}) was solubilized in 0.1 mol L^{-1} $NaNO_3$ (also used as eluent), followed by filtration through cellulose acetate Millipore membranes with nominal pore sizes of 0.22 μm. Data were analyzed with the help of OmniSEC software (Viscotek).

2.4. GAD chemical characterization

The polysaccharide sample (GAD) was hydrolyzed with 1 mol L^{-1} TFA (trifluoroacetic acid) for 8 h at 100 °C. TFA was then removed by evaporation and the product was successively reduced with $NaBH_4$ (to pH 10) in a small volume of water and maintained for 12 h (Wolfrom & Thompson, 1963a,b). After, the solution was treated with a cationic resin (DOWEX 50WX8 hydrogen form) reaching pH 4, filtered and dried in a rotary evaporator. After being washed several times with methanol, the product was dried. The resulting alditol were acetylated with Ac_2O–pyridine (1:1, v/v) (Wolfrom & Thompson, 1963a,b), and the resulting alditol acetates were examined by GC–MS. This was performed with a Varian model 3800 gas chromatograph coupled to a Saturn 2000R mass spectrometer using a DB-225 capillary column (25 m × 0.25 mm i.d.). Temperature used was 50 °C during injection, then programmed at 40 °C min^{-1} to 220 °C (constant), with He as carrier gas. The protein and uronic acids content of the polysaccharide were determined by the colorimetric methods described by Hartree (1972) and Filisetti-Cozzi and Carpita (1991), respectively. ^{13}C NMR spectra were obtained from solutions in D_2O at 50 °C, using a 400 MHz Bruker DRX Avance spectrometer equipped with a 5 mm inverse probe. Chemical shifts are expressed in δ ppm relative to an internal standard of acetone (δ 30.2).

Methylation of GAD was carried out according to Ciucanu and Kerek (1984). 5 mg of the sample were solubilized in Me_2SO followed by addition of powdered NaOH and CH_3I. Each mixture was agitated strongly for 30 min and then left for 18 h (Simas et al., 2004). After this, the mixture was neutralized with HOAc, dialysed (cut off 6–8 KDa) and freeze-dried. The procedure described above was carried out again. The per-*O*-methylated products were extracted with $CHCl_3$ from aqueous solutions and were hydrolyzed with 50% v/v H_2SO_4 (0.5 mL) at 0 °C for 1 h, followed by dilution to 5.5% v/v. The solution was maintained at 100 °C for 8 h (Saeman, Moore, Mitchell, & Millet, 1954). After hydrolysis, solutions were successively neutralized ($BaCO_3$), reduced with $NaBH_4$, and acetylated, as described above, to give a mixture of partially *O*-methylated alditol acetates, which were analyzed by GC–MS (DB-225 capillary column with 25 m × 0.25 mm i.d.). Temperatures employed were 50 °C during injection then programmed at 40 °C min^{-1} to 215 °C (constant), this temperature being maintained at 215 °C for 40 min. The partially-*O*-methylated alditol acetates were identified by their typical retention times and electron impact spectra (Sassaki, Gorin, Souza, Czelusniak, & Iacomini, 2005). The same procedures were conducted to study the sample GA and the results are published elsewhere (Grein et al., 2013).

2.5. Preparation of GA-PANI and GAD-PANI nanocomposites

The composites GA-PANI and GAD-PANI were obtained by the oxidation of aniline with ammonium persulfate (APS) in aqueous medium, according to a method adapted from the one proposed by Amarnath, Palaniappan, Rannou, and Pron (2008). For this, 0.5 g of GA or GADS were solubilized in 35 mL of distilled water and left overnight at 4 °C to ensure complete hydration. Under constant magnetic stirring, 3 mL of H_2SO_4 solution (1.7 mol L^{-1}), 1 mL of aniline (0.17 mol L^{-1}) and 35 mL of distilled water were added. The pH was then adjusted to 2.0, and at each 30 min, 200 μL of a solution of sodium persulfate (0.15 mol L^{-1}) were added. The syntheses were done at 35 °C and the formation of PANI was monitored by UV–vis spectroscopy (Agilent model 8453) through the observation of the bands at around λ_{max} = 400 nm and 750 nm (Stejskal, Kratochvil, & Radhakrishnan, 1993). The oxidizing agent was added until the observation of two consecutive and coincident values of λ_{max} and absorbance intensity. The reaction took around 210 min for completion. For comparison studies, exactly the same procedure was conducted in a batch in the absence of GA or GAD and another in the absence of aniline. The resulting GA-PANI and GAD-PANI dispersions were dialysed against distilled water for 24 h (1200–2000 Da cut-off) for removal of unreacted reagents, short oligomers and low molecular weight dissolved ions.

2.6. Characterization of GA-PANI and GAD-PANI nanocomposites: Raman vibrational spectroscopy and transmission electron microscopy

Samples were separated by centrifugation and dried at room temperature under reduced pressure prior to the Raman experiments. A Witec Alpha 300R equipment was employed, operating at a wavelength of 632.8 nm, with a resolution of 0.02 cm^{-1}.

The morphology of the composites was investigated by transmission electron microscopy (TEM), using a JEOL 1200EX-II microscope, and working at an acceleration voltage of 80 kV. A drop (~10 μL) of the colloidal solution was deposited onto 400 mesh grids, coated with Formar, and air dried. Size and size distribution of GA-PANI and GAD-PANI were determined using ImageJ and OriginPro 8 software, respectively.

Table 1
Monosaccharide composition, protein content and molecular weight of GA and GAD.

Sample	Monosaccharide composition (%)[a]					Protein content[c] (%)	$\bar{M}_w$ (g mol^{-1})
	Rha	Ara	Gal	Glc	Uronic acid[b]		
GA[d]	13	31	39	tr.	17.0 ± 0.7	3.6 ± 0.1	93.2×10^4
GAD	7	27	60	–	5.9 ± 0.1	7.9 ± 0.1	39.1×10^4

[a] Relative percentage of monosaccharides. Analyzed with a DB-225 column by GC–MS after acid hydrolysis, reduction, and acetylation.
[b] Determined by the colorimetric methods of Filisetti-Cozzi and Carpita (1991).
[c] Determined by the colorimetric methods of Hartree (1972).
[d] From Grein et al. (2013).

2.7. Electrochemical behavior

ITO (indium tin oxide) electrodes (Delta technologies, sheet resistance <12 Ω □$^{-1}$, 25 Ω cm^{-2}; 0.35 cm^{-2}) were modified by electrophoretic deposition (EPD) process. The cell was assembled by placing the ITO parallel with a stainless steel foil away from each other by 4.0 mm. Colloidal GA-PANI or GAD-PANI dispersions were used from the reaction batch, just after synthesis (without drying) and the adjustment of the pH to 2.0. An electric field of −3.75 V cm^{-1} was applied by a Minipa MPS-303D source during different times. At pH 2.0 it is believed that the composites bear positive electrical charges due to PANI protonation. Then the modified electrodes were dried in desiccator under low pressure and room temperature. Electrochemical experiments were performed at a scan rate of 10 mV s^{-1}, from −0.2 to 1.0 V, in an Autolab PGSTAT 30 potentiostat and using Pt foil and Ag/AgCl/Cl$^-_{(sat)}$ as counter and reference electrode respectively.

3. Results

3.1. Characterization of GAD

GAD was characterized and the results were compared with what was previously reported by our group for GA (Grein et al., 2013). The data are summarized in Table 1. GA and GAD are both composed of Rha, Ara, Gal and uronic acids in 13:31:39:17 and 7:27:60:6 molar ratios and contain around 4% and 8% of protein, respectively.

By size exclusion chromatography, we have previously found for GA a weight average molecular mass, $\bar{M}_w$, of 93.2×10^4 g mol^{-1}, a polydispersity index of 1.7 and evidences that the proteinaceous content corresponds mainly to the arabinogalactan-protein (AGP) fraction (Grein et al., 2013). Fig. 2 displays the GPC profiles of the samples GA and GAD. Important differences were evidenced as follows. The signals of RI and LS detectors reveal that the degradation process lowered the weight average molecular mass to 39.1×10^4 g mol^{-1} and increased the polydispersity. By RALS detector, it is demonstrated that GAD has no tendency to aggregate, as seen by the low value of the signal which is not the case for GA. Therefore, the applied degradation method has efficiently changed the molecular characteristics of GA.

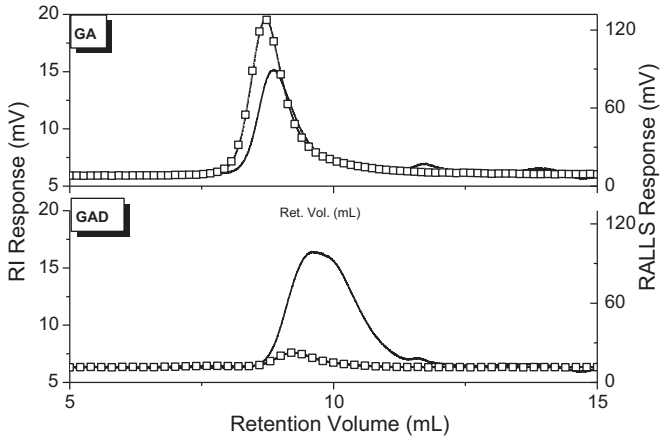

Fig. 2. GPC/SEC elution profiles of samples GA and GAD using refractive index (RI) (___) and right angle laser light scattering (RALLS) (-□-) detectors.

As expected, the controlled Smith degradation produced a less complex polysaccharide structure, as could be observed by the methylation data. Monosaccharides presenting adjacent hydroxyl groups such as nonreducing end-units of Gal*p*, Ara*f*, Glc*p*A, and Rha*p*, Gal*p*-6-*O*-linked units, and Glc*p*A-4-*O*-linked units were oxidized by periodate. However, units such as Gal*p*-3-*O*-, Gal*p*-3,6- and 3,4-di-*O*-, Gal*p*-3,4,6-tri-*O*-, and Ara*f*-3-*O*-linked were not oxidized (Scheme 1). Methylation data of GAD (Table 2), when compared with those previously obtained for GA (Grein et al., 2013), showed an increase in derivatives corresponding to Gal units 3-*O*- (13%), 6-*O*- (23%), and 3,6-di-*O*-substituted (26%) with proportional decrease of non-reducing end units of Ara*f* (16%), Gal*p* (7%) and of 3-*O*-substituted Ara*f* units (10%). These data indicates the obtention of a less branched structure composed mainly by Gal*p* (3-*O*-, 6-*O*-, and 3,6-di-*O*-substituted).

The ^{13}C NMR spectrum (Fig. 3) of GAD is in agreement with the methylation data. It shows C-1 signals at δ 109.3 and δ 109.1 corresponding to (1 → 3)-linked and non-reducing end of residual α-L-Ara*f* units (Simas et al., 2004; Delgobo, Gorin, Tischer, & Iacomini, 1999) still present in the structure. Signals at δ 103.9, δ 103.5, and δ 103.2 were attributed to C-1 of non-reducing end-, mono-, and di-*O*-substituted β-Gal*p* units, respectively (Agrawal, 1992; Delgobo, Gorin, Tischer, & Iacomini, 1999). Signals at δ 102.9 and δ 101.5 can be assigned to C-1 of β-Glc*p*A (Grein et al., 2013) and α-Rha*p* units (Gorin & Mazurek, 1975; Tischer et al., 2002), respectively, still present in GAD structure, agreeing with monosaccharide composition (Table 1).

Taking into account the previous and the present results, we propose an approximate scheme for the molecular structure of GA and GAD, which is presented in Scheme 1. The GAD showed a less branched structure and less complex side-chains than those founded for GA. The oxidation susceptible residues at GA structure are indicated by arrows, which can explain the residual structure of GAD.

3.2. GA-PANI and GAD-PANI nanocomposites

Aniline was polymerized by chemical oxidation, using APS as oxidant in aqueous medium, in the presence of either GA or GAD. UV–vis spectra were recorded at determined time intervals, after the addition of aliquots of the oxidizing agent, in order to follow the course of the polymerization. The PANI formation, in an acidic environment, in the presence of either GA or GAD, was evidenced by the increase in the absorption of the bands centered at, approximately, 400 and 750 nm, as the oxidizing agent was added to the reaction batch, kept at 35 °C (data not shown here). As the reaction proceeded, the reaction medium turned from colorless

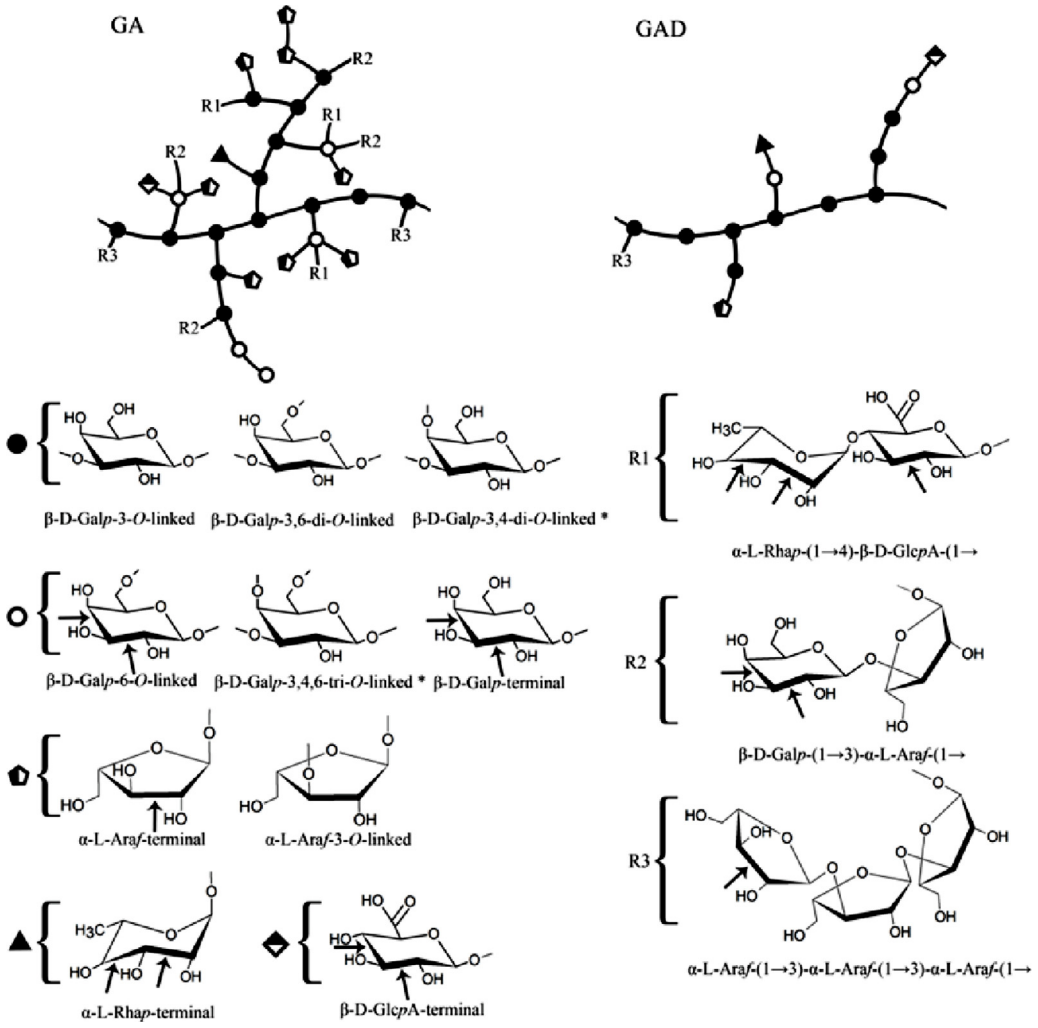

Scheme 1. GA* and GAD proposed structures based on monosaccharide composition analysis, methylation data, and ^{13}C NMR spectra. Arrows indicate possible points of cleavage by periodate oxidation. * Residues present at GA structure based on what was proposed by Phillips (Williams & Phillips, 2000) and on data previously reported by our group (Grein et al., 2013).

to emerald green. The spectra taken 30 min after the last addition of the oxidizing agent are available in the Supplementary data (Fig. S1). Although no modifications were found regarding the position of the peaks, their absorption intensities were clearly different when comparing GA-PANI and GAD-PANI. Since the absorption is related to the concentration of the analyzed material, we can infer that PANI is present in lower concentration when using GAD as stabilizer rather than GA.

The higher energy band, at 400 nm, is attributed to the polaronic form (cation radical) alongside PANI chains, whereas the peak centered at 750 nm evidences the excitonic transition of the quinoid rings, related to the bipolaronic state of PANI (Quintanilha

Table 2
Partially *O*-methylalditol acetates formed on methylation analysis of fractions GA and GAD.

Partially *O*-methylated alditol acetates[a]	Linkage types	(mol%)	
		GA[b]	GAD
2,3,5-Me_3-Ara2,3,4-Me_3-Rha	Araf-(1→Rhap-(1→	24*	16*
2,3,4-Me_3-Ara	Arap-(1→	3	–
3,5-Me_2-Ara	→2)-Araf-(1→	3	3
2,5-Me_2-Ara	→3)-Araf-(1→	18	9
2,3,4,6-Me_4-Gal	Galp-(1→	18	7
2,4,6-Me_3-Gal	→3)-Galp-(1→	4	13
2,3,4-Me_3-Gal	→6)-Galp-(1→	3	23
2,6-Me_2-Gal	→3,4)Galp-(1→	3	tr.
2,4-Me_2-Gal	→3,6)Galp-(1→	15	26
2-Me-Gal	→3,4,6)Galp-(1→	9	tr.

* The derivative 2,3,5-Me_3-Ara was overlapped with 2,3,4-Me_3-Rha in both fractions.
[a] Eluted successively from a DB-225 capillary column at 215 °C after hydrolysis, reduction, and acetylation.
[b] Grein et al. (2013).
tr: traces (<1%).

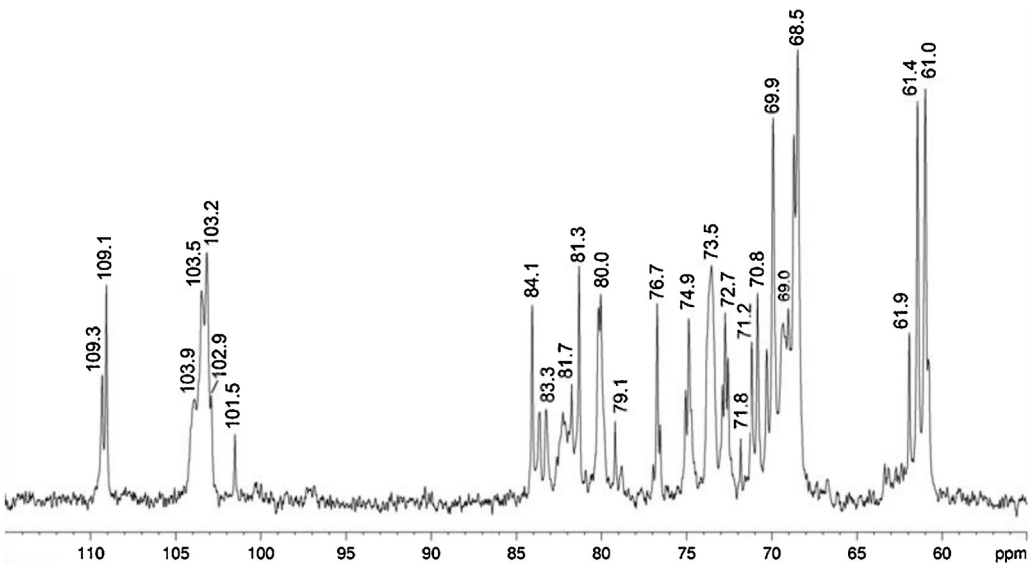

Fig. 3. ^{13}C NMR spectrum of the degraded Smith polysaccharide (GAD) in D_2O at 70 °C. Chemical shifts are expressed as δ ppm.

et al., 2014). Therefore, the increase in the absorption values at 400 and 750 nm indicates the polymerization of aniline towards the formation of PANI in its protonated conductive form. It is worth mentioning that GA, GAD and aniline alone do not absorb at 400 or 750 nm (Supplementary data—Fig. S2). The dispersions remained stable for at least one week, when stored at 5 °C, as seen by the absence of precipitates. The determination of the zeta potential (ζ) of the particles confirmed that GA sample has lost glucuronic acid units, which were located in the non-reducing ends and as 4-*O*-substituted units (Supplementary data—Fig. S3).

Raman spectroscopy is a well established technique for investigating the macromolecular characteristics of PANI (Cochet, Louarn, Quillard, Buisson, & Lefrant, 2000b). The Raman spectrum is sensitive to PANI molecular properties, oxidation state and doping process. The bands above 1000 cm^{-1} are attributed to the in-plane vibration modes and in the low frequency region (below 1000 cm^{-1}) the out-of-plane vibrations are evidenced (Cochet et al., 2000a).

Fig. 4 shows the Raman spectra of the as-synthesized solid composites, GA-PANI and GAD-PANI, collected at 632.8 nm laser wavelength. At the selected wavelength, the vibrational modes corresponding to the oxidized portions of the polymer are enhanced. Neat-PANI was synthesized under the very same conditions, in the absence of GA or GAD, and studied accordingly. In the entire frequency range, it is evident the higher complexity of the composites' spectra when compared with neat-PANI.

All spectra shown in Fig. 4 present typical vibration bands assigned to PANI, however, different profiles are occasionally observed when comparing the samples. The bands at 410 cm^{-1} and 513 cm^{-1} are attributed to out-of-plane C—H wag and out-of-plane C—N—C torsion of bipolaronic structures (Cochet et al., 2000a), being very sensitive to the conformation of the chains. The first band is slightly broader in neat-PANI and GAD-PANI than in GA-PANI and the second is shifted to higher frequencies in neat-PANI, indicating differences in the conformation of the PANI chains due the presence of the polysaccharides. The bands at 579 cm^{-1} and at 1375 cm^{-1} are attributed to the vibration modes of tertiary amines, which are present as phenazyne segments in crosslinked PANI chains (Silva, Temperini, & Torresi, 2005) They are clearly evident for neat-PANI, less intense for GAD-PANI and appear as a shoulder in GA-PANI, indicating that, despite presenting higher protein content (Table 1), GAD interacts less efficiently with PANI. Associated with the previous bands, is the band at 608 cm^{-1} (in plane benzene deformation) that appears with low intensity in neat-PANI and as a well defined band in the composites. So, the crosslinked state of PANI chains can be corroborated by the hindering of the vibration modes of the benzene rings. These observations are indicative that the presence of the polysaccharides prevents the reaction between two adjacent PANI chains. This effect is more pronounced for GA-PANI, since no evidence of phenazine fragments was observed. In the GAD-PANI, the presence of few fragments of crosslinked structures can be suggested by the lower OH content in the GAD as it is a less branched structure if compared with GA. Due to the hydrogen bonds, the amine sites of PANI are specially surrounded by the polysaccharide and in the GAD composites, the protection of the NH sites from crosslink reactions is not so effective as found in the GA-PANI, but satisfactorily higher when compared with neat-PANI.

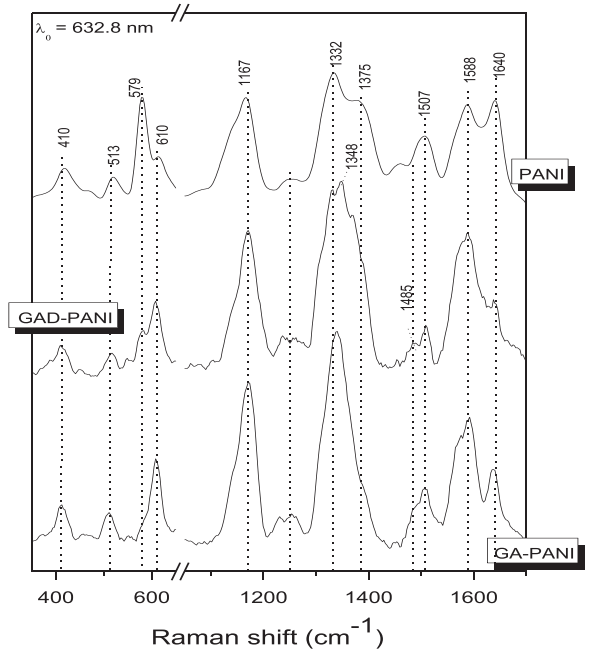

Fig. 4. Raman spectra for GA-PANI and GAD-PANI, obtained at 632.8 nm. The spectrum of neat-PANI is shown for comparison.

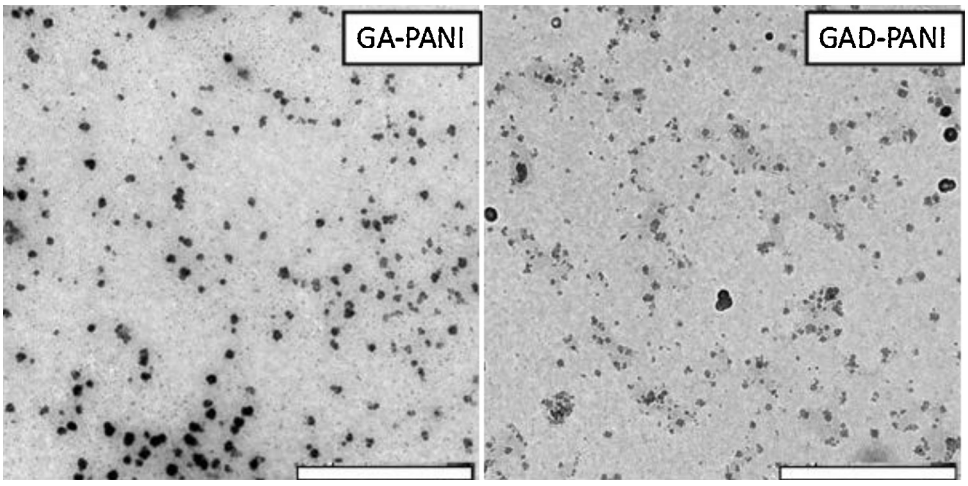

Fig. 5. Representative TEM images for the GA-PANI and GAD-PANI. Scale bars: 2 μm.

The band with maximum at 1167 cm^{-1} is associated with C—H bending of quinoid rings. An intense band at 1167 cm^{-1} is present in all samples, occurring as a large band for neat-PANI and more intense and well defined mode in the composites, indicating a higher occurrence of quinoid structures in the composites. The band centered at 1332 cm^{-1} can be attributed to the C—N vibrational modes and at high level of doping this band is normally found at higher frequencies, indicating the presence of $C—N^{\bullet+}$, polaronic structure (Salvatierra, Oliveira, & Zarbin, 2010). Interestingly the GAD-PANI sample presents a doublet at 1332 and 1348 cm^{-1}. On the other hand, this band is slight shifted in the GA-PANI sample. According to Silva, Temperini, and de Torresi (1999), the presence of organic acids leads to the secondary doping effect of PANI, with an increase of conductivity due to specific conformational changes indicated by the presence of semiquinone unities, characterized by the diminishment of the 1332 cm^{-1} band, corroborating the results presented herein.

The presence of hydrogen bonds interaction between the polysaccharides and PANI can also be evidenced by the band at 1507 cm^{-1} which is attributed to NH bending (Cochet et al., 2000a). In neat-PANI, a broad band is observed whereas in GAD-PANI and GA-PANI this band is more defined, indicating that this vibrational mode is being influenced by the surrounding structures. This fact can be attributed to the presence of the polysaccharides, specifically by the OH groups which interact with the amine group presented in the PANI structure, this interaction is strong enough to keep the composite integrity (Eiras et al., 2007; Cheng, Xia, & Chan, 2005; Quintanilha et al., 2014).

In all samples, the band at 1588 cm^{-1} is attributed to C—C stretching of intermediate structures between quinoid and semiquinoid rings and the band at 1640 cm^{-1} is attributed to C—C stretching of benzenoid rings. In neat-PANI those bands appear with nearly the same intensity whereas in the composites the first one (at 1588 cm^{-1}) is clearly more intense, corroborating the presence of highly doped PANI structures, mainly polaronic ones, in the composites (Cochet et al., 2000a,b; Silva et al., 2005; Salvatierra et al., 2010).

TEM images were obtained in order to investigate the shape and size of the composites. As shown in Fig. 5, small and large particles are seen in both samples, being the larger ones probably corresponding to aggregates. Particles are nearly spherical, although perfectly spheres were rarely seen. The size distribution curves, and the best Gaussian fit reveal an average diameter of 91.0 ± 10.5 nm and 59.5 ± 5.5 nm for GA-PANI and GAD-PANI, respectively. Considering the higher complexity of GA chains and its tendency of to aggregate in solution (See Scheme 1 and Fig. 1), a larger number of aniline molecules will possibly adsorbs to GA rather than to GAD, thus leading to larger PANI particles (which is in accordance with the UV–vis results, **Fig. S1**). Even though, at this situation, PANI chains are prevented to reticulate, as seen by Raman spectroscopy, thus suggesting that GA molecules are interpenetrated through PANI chains. Higher magnification images did not demonstrate phase separation between PANI and GA or GAD, since spherical and homogeneous objects were always seen (up to 70k). It is worth mentioning that TEM images of free polysaccharides were tentatively obtained. However, due to the low contrast, it was not possible to elucidate any distinct morphological feature between the polysaccharides. Therefore, it can be concluded that compact nanocomposites were produced, comprising intimate contact between the constituent polymers.

The electrochemical behavior of both composites when deposited onto ITO surfaces by EPD was investigated. The electroactivity was evaluated by cyclic voltammetry. The electrochemical behavior of thin films of PANI is vastly described in literature and two different process can be described, the conversion from leucoemeraldine base/emeraldine salt and emeraldine salt/pernigraniline, in aqueous solution. The well-defined oxidation peaks of the corresponding reactions occur at ca. 0.20 V and 0.75 V (vs Ag/AgCl), respectively, and strongly depend on the proton diffusional processes through ion/out the polymer. The position and the format of the voltammetric peaks change according to the employed electrolyte, i.e. $LiClO_4$, tetrabutyl ammonium, camphorsulfonic acid, and for larger species, in most cases, the two PANI redox reactions overlap in a unique voltammetric wave. So, both, electrolyte and electrode modification affect the PANI electrochemical behavior. EPD offers very interesting advantages over other deposition techniques as the nanometric electroactive material is directly adsorbed onto the electrode surface and the nanometric structure is readily maintained (Vidotti & de Torresi, 2009).

In Fig. 6 are shown the voltammetric behavior of GAD-PANI and GA-PANI modified electrodes. It is important to mention that the deposition occurred at pH 3 where the functional groups of GA and PANI are preferentially protonated (Blinova, Sapurina, Klimovic, & Stejskal, 2005) providing a positive net charge to the macromolecules. Both electrodes showed the traditional PANI electroactive behaviour with observable redox processes corresponding to leucoemeraldine/emeraldine (around 0.20/0.05 V) and emeraldine/pernigraniline (around 0.75/0.63 V). The net charge passing through the GA-PANI electrode is higher if compared with GAD-PANI electrode; this fact can be associated with the amount

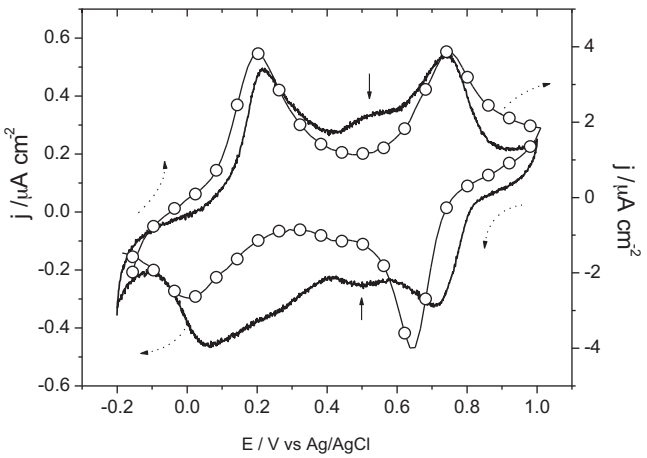

Fig. 6. Cyclic voltammograms performed for ITO electrodes modified by EPD, for 60 min, with GA-PANI (-○-) or GAD-PANI (---) composites. Electrolyte: H_2SO_4 0.05 mol L^{-1}, platinum and Ag/AgCl used as counter and reference electrodes, respectively.

of material on the electrode surface, with a consequent diminishment of the voltammetric charge. It is important to note that the motion and deposition of the particles on the electrode surface depends mainly to the relationship between electric charge and volume of the particles. Despite presenting higher particles, the GA-PANI composite deposited more efficiently to the electrode surface, possibly due to the more effective electric charge provided by the higher content of PANI chains in its structure, as seen in TEM images (Fig. 5).

Both voltammograms presented classic PANI behavior. However, in the case of GAD-PANI electrode an additional redox process appears around 0.45 V. Processes at this region is commonly related to the presence of phenazine segments alongside the polymer. This fact corroborates the Raman spectra and also provides important information on the effect of structural modification of stabilizing macromolecules. The presence of more complex lateral segments in GA is fundamental for the PANI integrity that has the effect of splitting apart parallel chains avoiding the reticulation and consequently resulting in better electrochemical performance.

4. Conclusions

Controlled Smith degradation was successfully employed to structurally modify gum arabic (GA), which is a highly branched acidic arabinogalactan. Both, native and modified samples (GA and GAD) acted as stabilizers during the synthesis of polyaniline (PANI) in aqueous medium. In the presence of GA or GAD, PANI presented distinct spectroscopic and electrochemical properties. In the composites, PANI is less reticulated and highly doped. However, the more complex polysaccharide, i.e. GA, was more efficient in preventing the occurrence of crosslinking between PANI chains, thus leading to PANI with the best electrochemical response. Considering the macromolecular and compositional features of both studied polysaccharides, it is possible to infer that the molecular mass and the degree of branching are the key factors that ensure the excellent performance of GA as stabilizer of hydrophobic polymers in aqueous dispersion.

Acknowledgements

The authors acknowledge the support given by the Brazilian National Counsel of Technological and Scientific Development (CNPq) mainly through the grants 577232/2008-8, 477467/2010-5 and 564741/2010-8 (Rede Nanoglicobiotec). F. F. Simas-Tosin acknowledges the pos-doctoral fellowship (PNPD/CNPq—558550/2008-8). P. A. Cornelsen and R. C. Quintanilha express their gratitude to CAPES for the fellowships. Authors would like to thank Prof[a]. Maria Rita Sierakowski (BioPol/UFPR) for GPC/SEC facilities (CNPq, 555169/2005-7) and Dr. Mateus Borba Cardoso (LNLS-Brazilian Synchrotron Light Laboratory) for the Zeta potential measurements (Fapesp—project number: 2011/21954-7). Also, the authors are very grateful to the Electron Microscopy Center of UFPR (CME-UFPR) for the TEM images and the Raman spectra.

Appendix A. Supplementary data

Supplementary data associated with this article can be found, in the online version, at http://dx.doi.org/10.1016/j.carbpol.2014.11.020.

References

Agrawal, P. K. (1992). NMR-spectroscopy in the structural elucidation of oligosaccharides and glycosides. *Phytochemistry*, *31*, 3307–3330.
Amarnath, C. A., Palaniappan, S., Rannou, P., & Pron, A. (2008). Acacia stabilized polyaniline dispersions: Preparation, properties and blending with poly(vinyl alcohol). *Thin Solid Films*, *516*, 2928–2933.
Ates, M. (2013). A review study of (bio)sensor systems based on conducting polymer. *Material Science and Engineering C*, *33*, 1853–1859.
Blinova, N. V., Sapurina, I., Klimovic, J., & Stejskal, J. (2005). The chemical and colloidal stability of polyaniline dispersions. *Polymer Degradation and Stability*, *88*, 428–434.
Cheng, D., Xia, H., & Chan, H. S. O. (2005). Synthesis and characterization of surface-functionalized conducting polyaniline-chitosan nanocomposite. *Journal of Nanoscience and Nanotechnology*, *5*, 474–481.
Cipriani, T. R., Mellinger, C. G., Gorin, P. A. J., & Iacomini, M. (2004). An arabinogalactan isolated from the medicinal plant *Maytenus ilicifolia*. *Journal of Natural Products*, *67*, 703–706.
Ciucanu, I., & Kerek, F. (1984). A simple and rapid method for the permethylation of carbohydrates. *Carbohydrate Research*, *131*, 209–217.
Cochet, M., Louarn, G., Quillard, S., Boyer, M. I., Buisson, J. P., & Lefrant, S. (2000). Theoretical and experimental vibrational study of emeraldine in base form: Non-planar analysis. Part I. *Journal of Raman Spectroscopy*, *31*, 1029–1039.
Cochet, M., Louarn, G., Quillard, S., Buisson, J. P., & Lefrant, S. (2000). Theoretical and experimental vibrational study of emeraldine in salt form. Part II. *Journal of Raman Spectroscopy*, *31*, 1041–1049.
Delgobo, C. L., Gorin, P. A. J., Tischer, C. A., & Iacomini, M. (1999). The free reducing polysaccharides of angico branco (*Anadenanthera colubrina*) gum exudate: An aid for structural assignments in the heteropolysaccharide. *Carbohydrate Research*, *320*, 167–175.
Duffus, C. M., & Duffus, J. H. (1984). *Carbohydrate metabolism in plants*. New York, NY: Longman.
Eiras, C., Passos, I. N. G., de Brito, A. C. F., dos Santos, J. R., Zucolotto, V., Oliveira, O. N., Kitagawa, I. L., Constantino, C. J. L., & da Cunha, H. N. (2007). Electroactive nanocomposites made of poly(*O*-methoxyaniline) and natural polysaccharides. *Quimica Nova*, *30*, 1158–1162.
Ferrier, R. J., & Collins, P. M. (1972). *Monosaccharide chemistry*. London: Penguin Books.
Filisetti-Cozzi, T. M. C. C., & Carpita, N. C. (1991). Measurement of uronic acids without interference from neutral sugars. *Analytical Biochemistry*, *197*, 157–162.
Goldstein, I. J., Hay, G. W., Lewis, B. A., & Smith, F. (1965). Controlled degradation of polysaccharides by periodate oxidation, reduction and hydrolysis. In R. L. Whistler, & M. L. Wolfrom (Eds.), *Methods in carbohydrate chemistry* (5) (pp. 361–369). New York, NY: Academic Press.
Gorin, P. A. J., Horitsu, K., & Spencer, J. F. T. (1965). An exocellular mannan alternately linked 1,3-β and 1,4-β from *Rhodotorula glutinis*. *Canadian Journal of Chemistry*, *43*, 950–954.
Gorin, P. A. J., & Mazurek, M. (1975). Further studies on assignment of signals in ^{13}C magnetic resonance spectra of aldoses and derived methyl glycosides. *Canadian Journal of Chemistry*, *53*, 1212–1224.
Grein, A., Silva, B. C., Wendel, C. F., Tischer, C. A., Sierakowski, M-R., Moura, A. B. D., Iacomini, M., Gorin, P. A. J., Simas-Tosin, F. F., & Riegel-Vidotti, I. C. (2013). Structural characterization and emulsifying properties of polysaccharides of *Acacia mearnsii* de Wild gum. *Carbohydrate Polymers*, *92*, 312–320.
Guo, B., Glavas, L., & Albertsson, A-N. (2013). Biodegradable and electrically conducting polymers for biomedical applications. *Progress in Polymer Science*, *38*, 1263–1286.
Hartree, E. F. (1972). Determination of protein: A modification of the Lowry method that gives a linear photometric response. *Analytical Biochemistry*, *48*, 422–427.
Hay, G. W., Lewis, B. A., & Smith, F. (1965). Periodate oxidation of polysaccharides: General procedures. In R. L. Whistler, & M. L. Wolfrom (Eds.), *Methods in carbohydrate chemistry* (vol. 5) (pp. 357–360). New York, NY: Academic Press.

Islam, A. M., Phillips, G. O., Sljivo, A., Snowden, M. J., & Willians, P. A. (1997). A review of recent developments on the regulatory, structural and functional aspects of gum arabic. *Food Hydrocolloids*, *11*, 493–505.

Janáky, C., & Visy, C. (2013). Conducting polymer-based hybrid assemblies for electrochemical sensing: A materials science perspective. *Analytical and Bioanalytical Chemistry*, *405*, 3489–3511.

Palaniappan, S., & John, A. (2008). Polyaniline materials by emulsion polymerization pathway. *Progress in Polymer Science*, *33*, 732–758.

Petrov, P., Georgiev, G., Momekova, D., Momekov, G., & Tsvetanov, C. B. (2010). UV-assisted grafting of polymers: A method towards biocompatible carbon nanotube. *Polymer*, *51*, 2465–2471.

Quintanilha, R. C., Orth, E. S., Grein-Iankovski, A., Riegel-Vidotti, I. C., & Vidotti, M. (2014). The use of gum Arabic as "Greenstabilizer of poly(aniline) nanocomposites: A comprehensive study of spectroscopic, morphological and electrochemical properties. *Journal of Colloid and Interface Science*, *434*, 18–27.

Saeman, J. F., Moore, W. E., Mitchell, R. L., & Millet, M. A. (1954). Techniques for the determination of pulp constituents by quantitative paper chromatography. *Technical Association of the Pulp and Paper Industry*, *37*, 336–343.

Salvatierra, R. V., Oliveira, M. M., & Zarbin, A. J. G. (2010). One-pot synthesis and processing of transparent, conducting, and freestanding carbon nanotubes/polyaniline composite films. *Chemistry of Materials*, *22*, 5222–5234.

Sassaki, G. L., Gorin, P. A. J., Souza, L. M., Czelusniak, P. A., & Iacomini, M. (2005). Rapid synthesis of partially *O*-methylated alditol acetate standards for GC–MS: Some relative activities of hydroxyl groups of methyl glycopyranosides on Purdie methylation. *Carbohydrate Research*, *340*, 731–739.

Shi, Z., Phillips, G. O., & Yang, G. (2013). Nanocellulose electroconductive composites. *Nanoscale*, *5*, 3194–3201.

Silva, J. E. P., Temperini, M. L. A., & de Torresi, S. I. C. (1999). Secondary doping of polyaniline studied by resonance Raman spectroscopy. *Electrochimica Acta*, *44*, 1887–1891.

Silva, J. E. P., Faria, D. L. A., de Torresi, S. I. C., & Temperini, M. L. A. (2000). Influence of thermal treatment on doped polyaniline studied by resonance Raman spectroscopy. *Macromolecules*, *33*, 3077–3083.

Silva, J. E. P., Temperini, M. L. A., & de Torresi, S. I. C. (2005). Characterization of conducting polyaniline blends by resonance Raman spectroscopy. *Journal of the Brazilian Chemical Society*, *16*, 322–327.

Simas, F. F., Gorin, P. A. J., Guerrini, M., Nagi, A., Sassaki, G. L., Delbogo, C. L., & Iacomini, M. (2004). Structure of a heteroxylan of gum exudate of the palm *Scheelea phalerata* (urucuri). *Phytochemistry*, *65*, 2347–2355.

Stejskal, J., Kratochvil, P., & Radhakrishnan, N. (1993). Polyaniline dispersions 2. UV–vis absorption spectra. *Synthetic Metals*, *61*, 225–231.

Stejskal, J., & Sapurina, I. (2004). On the origin of colloidal particles in the dispersion polymerization of aniline. *Journal of Colloid and Interface Science*, *274*, 489–495.

Tischer, C. A., Gorin, P. A. J., & Iacomini, M. (2002). The free reducing oligosaccharides of gum arabic: Aids for structural assignments in the polysaccharide. *Carbohydrate Polymers*, *47*, 151–158.

Vidotti, M., & de Torresi, S. I. C. (2009). Electrostatic layer-by-layer and electrophoretic depositions as methods for electrochromic nanoparticle immobilization. *Electrochimica Acta*, *54*, 2800–2804.

Wang, B., Wang, L-J., Dong, L., Adhikaric, B., & Shid, J. (2011). Effect of gum arabic on stability of oil-in-water emulsion stabilized by flaxseed and soybean protein. *Carbohydrate Polymers*, *86*, 343–351.

Williams, P. A., & Phillips, G. O. (2000). Gum arabic. In G. O. Phillips, & P. A. Williams (Eds.), *Handbook of food hydrocolloids*. England: CRC Press (Ch 9)

Wolfrom, M. L., & Thompson, A. (1963a). Reduction with sodium borohydride. In R. L. Whistler, & M. L. Wolfrom (Eds.), *Methods in carbohydrate chemistry* (2) (pp. 65–68). New York: Academic Press.

Wolfrom, M. L., & Thompson, A. (1963b). Acetylation. In R. L. Whistler, & M. L. Wolfrom (Eds.), *Methods in carbohydrate chemistry* (2) (pp. 211–215). New York: Academic Press.